frontiers in Energy Research

ORIGINAL RESEARCH
published: 18 March 2022
doi: 10.3389/fenrg.2022.828978

Control of Boost Converter Using Observer-Based Backstepping Sliding Mode Control for DC Microgrid

Rifqi Firmansyah Muktiadji[1]*, *Makbul A. M. Ramli*[1,2], *Houssem R. E. H. Bouchekara*[3], *Ahmad H. Milyani*[1], *Muhyaddin Rawa*[1,2], *Mustafa M. A. Seedahmed*[1] and *Firmansyah Nur Budiman*[1]

[1]Department of Electrical and Computer Engineering, Faculty of Engineering, King Abdulaziz University, Jeddah, Saudi Arabia, [2]Center of Research Excellence in Renewable Energy and Power Systems, King Abdulaziz University, Jeddah, Saudi Arabia, [3]Department of Electrical Engineering, University of Hafr Al Batin, Hafr Al Batin, Saudi Arabia

The output voltage of a photovoltaic (PV) system relies on temperature and solar irradiance; therefore, the PV system and a load cannot be connected directly. To control the output voltage, a DC-DC boost converter is required. However, regulating this converter is a very complicated problem due to its non-linear time-variant and non-minimum phase circuit. Furthermore, the problem becomes more challenging due to uncertainty about the output voltage of the PV system and variation in the load, which is a non-linear disturbance. In this study, an observer-based backstepping sliding mode control (OBSMC) is proposed to regulate the output voltage of a DC-DC boost converter. The input voltage of the converter can be a DC energy source such as PV-based microgrid systems. An adaptive scheme and sliding mode controller constructed from a dynamic model of the converter is used to design an observer. This observer estimates unmeasured system states such as inductor current, capacitor voltage, uncertainty output voltages of the PV cell, and variation of loads such that the system does not need any sensors. In addition, the backstepping technique has been combined with the SMC to make the controller more stable and robust. In addition, the Lyapunov direct method is employed to ensure the stability of the proposed method. By employing the proposed configuration, the control performance was improved. To verify the effectiveness of the proposed controller, a numerical simulation was conducted. The simulation results show that the proposed method is always able to accurately follow the desired voltage with more robustness, fewer steady-state errors, smaller overshoot, faster recovery time, and faster transient response time. In addition, the proposed method consistently produces the least value of integral absolute error.

Keywords: observer design, backstepping, sliding mode control, DC-DC boost converter, DC microgrid

OPEN ACCESS

Edited by:
Sudhakar Babu Thanikanti, Chaitanya Bharathi Institute of Technology, India

Reviewed by:
Minh Quan Duong, University of Science and Technology, Vietnam
Karthik Balasubramanian, McMaster University, Canada

***Correspondence:**
Rifqi Firmansyah Muktiadji
rifqifirmansyah@unesa.ac.id

Specialty section:
This article was submitted to Smart Grids, a section of the journal Frontiers in Energy Research

Received: *04 December 2021*
Accepted: *31 January 2022*
Published: *18 March 2022*

Citation:
Muktiadji RF, Ramli MAM, Bouchekara HREH, Milyani AH, Rawa M, Seedahmed MMA and Budiman FN (2022) Control of Boost Converter Using Observer-Based Backstepping Sliding Mode Control for DC Microgrid. Front. Energy Res. 10:828978. doi: 10.3389/fenrg.2022.828978

INTRODUCTION

The development of small renewable energy sources (RES) integrated into the power system has significantly increased since the last decade as an effort to boost global penetration of such energy sources. As alternative energy sources, RES are implemented within localized grids, which are called microgrids, that can be disconnected from the main grid whenever needed. These microgrids can be implemented in the form of AC and DC microgrid coupled with power converter. The intensive use of DC-based renewable energy and electronic DC loads (e.g., electric vehicle and data center) have

made DC microgrids option more efficient (Mahajan and Potdar, 2020). The DC microgrid has several benefits such as improved reliability, high efficiency with less energy conversion, high controllability without synchronization problem, and economics (Saveen et al., 2018). Moreover, DC microgrids can avoid problems in AC microgrids such as power quality issues, reactive power flow, and frequency synchronization (Abhinav et al., 2019). In the DC microgrid, the DC energy source such as PV, fuel cell, and battery is connected to the DC bus through a DC-DC boost converter (Balog et al., 2012). Nowadays, DC-DC converters are developing quickly and widely being applied in renewable energy sources, power grids, DC motor drives, uninterruptible power supply, computers, data communications, and other fields (Toumi et al., 2021; Vazquez et al., 2017). This motivates to improve converters to be more reliable (Yu et al., 2012), high quality (Alsolami 2021), efficient (Eguchi et al., 2020), and well controlled (Li et al., 2021). There are several DC-DC converter topologies, such as the boost type (Chen et al., 2020), buck type (Basharat et al., 2021), buck-boost type (Yang et al., 2020), Cuk type (Ramos-Paja, et al., 2020), and zeta type converter (Arun and Manigandan, 2021). Among these topologies, the boost type is widely used in many industrial applications (Amirabadi 2016). Generally, a DC-DC boost converter is utilized to convert the DC voltage to a higher DC voltage (Premkumar et al., 2019).

The DC-DC boost converter is well known as a variable structure in a non-linear (Cajamarca et al., 2019), non-minimum phase (Tahri et al., 2019) and time-varying system (Zhang et al., 2017). Disturbance from load variation, input voltage uncertainty, and interference of electromagnetism created by the switching action of the semiconductor make the problem of the converter more challenging (Liu et al., 2018). Moreover, regulating the output voltage cannot be carried out directly without involving the inductor current (Bouchekara et al., 2021). Thus, the system requires a sensor to continuously measure the current (Shen et al., 2021); however, installing the sensor can make the system quite vulnerable to disturbance and raise construction costs (Abdelmalek et al., 2020). Therefore, to reach a suitable control performance for the system, a high-performance control is needed to have good disturbance rejection, less steady-state error, small overshoot, a fast recovery time, and fast transient response time (Mehdi et al., 2020; Mobayen and Tchier, 2018). In addition, the observer method is proposed for induction current estimation, meaning no sensor is needed for real-time measurement (Mehreganfar et al., 2019).

In the literature, many different control techniques have been introduced to control the output voltage of boost converters such as proportional-integral (PI) and proportional-integral-derivative (PID). In Guo et al. (2011), linear PID and PI controllers are used to control the boost converter with a DSP-based digital controller. The results of this study indicate that the PID and PI controllers are slow to achieve transient response with a big overshoot during startup, being less stable, and less robust against operating point changes. Kobaku et al. (2021a) investigated the problem of disturbance rejection for a non-minimum phase DC-DC boost converter employing a novel robust PID. The equivalent feedforward technique of the modified direct synthesis is used to build the controller. The results indicated that the proposed technique has robust performance and provides a fast recovery to the reference in the presence of disturbances. Another study (Cisneros et al., 2015) evaluated a linear time-varying PI controller for an interleaved boost and multilevel converter, while Ahmed et al. conducted a design of fractional order PI for the PV system with a DC-DC boost converter (Mohamed et al., 2021). In other studies, robust control was proposed to regulate boost converter (Mushi et al., 2017; Villegas-Ruvalcaba et al., 2021). Research results indicate that the proposed method shows good performance under different operating conditions. Moreover, Seo and Choi (2019) implemented a fractional order PID to regulate the DC-DC boost converter. In this research, input inductance and output capacitance values are used to characterize gains of integer order PID that will create a transfer function of the closed system equal to the first-order system. The results showed that the proposed technique is better than a conventional integer-order PID. Furthermore, the adaptive control technique was presented for controlling the boost converter, concluding that the driving voltage of the boost converter is controlled automatically (Alawieh et al., 2011; Johnson, et al., 2021). A quantitative feedback theory adapted to build a robust PID controller was proposed to address the problem of instability in voltage control of DC-DC boost converter. The results revealed that the proposed method is better than the conventional PID for various disturbances (Kobaku et al., 2021b). Moreover, Van et al. (2021) proposed phase shift full bridge to improve the output of DC-DC converter. The controller used in this study is PI controller. The results indicated that the phase shift full bridge converter has a better performance compared with other converters.

The aforementioned methods have a disadvantage. To obtain a control parameter, the controller needs a linearization in a certain operating point. Hence, the boost converter cannot achieve all conditions and operating range. To solve this problem, a non-linear controller using intelligent control techniques has been proposed. Nizami and Chakravarty (2020) presented an output voltage control problem for a DC-DC boost converter using a neural network integrated with an adaptive backstepping framework. The results obtained revealed the method is faster at estimating the unknown parameter and has satisfactory tracking of the output voltage. Wai et al. (2012) proposed an adaptive fuzzy neural network to control the voltage of a conventional boost converter. The results indicated that the proposed method is more suitable to control the voltage tracking of the boost converter. Moreover, in Guo and Abdul (2021), a fuzzy adaptive PSO controller was investigated to control maximum power point tracking (MPPT). The results revealed that the developed control method can enhance the global search process and raise the speed of convergence. A robust pulse width modulation-based type 2 fuzzy control to control DC-DC boost converter for improving the stability of converter is presented in Farsizadeh et al. (2020). However, the controller stability of intelligent control techniques cannot be investigated.

Another approach is employing the SMC method. Yuan et al. (2015) proposed the passive sliding mode to regulate the boost

converter. The simulation results showed that the proposed method has good dynamic, static performance and robustness against disturbance. Martínez-Treviño et al. (2017) presented an SMC of a boost converter to supply a constant power load and concluded that the technique has proven to be an effective solution to control the converter. Moreover, a new non-linear sliding surface form with optimal parameter to regulate DC-DC boost converter was presented by Yosra Massaoudi et al. (2013). It is concluded that the proposed method is more effective to eliminate chattering and has fast response. In other studies, an adaptive SMC for a load frequency control system based on disturbance observer was proposed (Wei et al., 2021), while Cucuzzella et al. (2018) conducted SMC to regulate the boost converter in a DC microgrid. Different from other methods, this can ensure the stability of the system design. In previous works, SMC was constructed based on observer design to consider disturbances from load variation and input voltage uncertainty (Oucheriah and Guo, 2013; Pandey et al., 2018), whereas in Pandey et al. (2020), the authors proposed two methods for estimating uncertainties of input voltage and load variation, namely, state observer–based adaptive law and sliding mode control, to regulate output voltage of the converter. The results indicate that the steady state and transient performance of the converter using the proposed method is satisfactory. Furthermore, Talbi et al. (2020) presented adaptive sliding mode observer for regulating boost converter using model predictive control and concluded that the proposed method can accurately estimate the output voltage of the converter. However, the recovery time due to the disturbance tends to slow the system and must be improved. To make the system more robust, backstepping SMC techniques are proposed in Xu et al. (2019). This technique is combined with a command filter to adjust the DC-link voltage. The simulation results show that the developed strategy can precisely regulate the grid-connected inverter. An adaptive backstepping sliding mode control method to enhance DC bus voltage stability is presented by Wu and Lu (2019). The results showed that the proposed control method has better performance and is more robust. In other studies, backstepping SMC was presented for maximum power point tracking in a solar cell (Bjaoui et al., 2019; Dahech et al., 2017) and concluded that the proposed technique has a good transient response, small tracking error, and very fast reaction against variations of solar irradiation. However, disturbance from load variation and input voltage uncertainty was not considered. Furthermore, observer design to estimate inductor current is not included in the SMC design. To the best of the authors' knowledge, no study has been conducted to design controller using a combination of observer-based backstepping technique and sliding mode control. In addition, to evaluate the performance of the proposed controller, most literature do not employ dynamic system testing for input voltage uncertainty and load variation.

In this paper, to improve the controller performance, observer-based backstepping sliding mode control (OBSMC) for regulating output voltage of DC-DC boost converter is proposed. The proposed controller will make the system performance more robust with less steady-state error, small overshoot, fast recovery time, and fast transient response time. The disturbance from load variation, input voltage uncertainty, and the estimation of the inductor current is considered in the design. The contributions of this paper are summarized as follows:

1. Combining the observer-based backstepping technique and sliding mode control and the mathematical model of DC-DC boost converter, a novel sliding surface is constructed. Then, using the Lyapunov method, the stability of the design is verified.
2. A novel controller formula is designed based on the novel sliding surface to regulate a DC-DC boost converter considering load variation and input voltage uncertainty.
3. The dynamic system testing for input voltage uncertainty and the load variation is applied to evaluate the performance of the controller.

The rest of this work is structured as follows. The mathematical modeling of the DC-DC boost converter is explained in **Section 2**. **Section 3** defines the OBSMC. In **Section 4**, the simulation results and analyses are discussed. Finally, conclusions are presented at the end of the study in **Section 5**.

MATHEMATICAL MODELING OF A DC-DC BOOST CONVERTER

To connect and regulate the output voltage of the PV system and a load, a DC-DC boost converter is required because the output voltage of a PV system relies on temperature and solar irradiance, as shown in **Figure 1**. Furthermore, due to the presence of an uncertain output voltage of the solar cell and variation of load, which is a non-linear disturbance, the controller technique is required to provide the gating signal pulse for regulating the DC-DC boost converter. To obtain the controller, the mathematical modeling of the converter is considered.

The circuit of a DC-DC boost converter, as presented in **Figure 2**, is a power electronic circuit comprising an inductor and a capacitor as energy storage to change one voltage level to another voltage level using a switching method, where the parameters of V_i, L, C, R, and V_0 are the input voltage, inductor, capacitor, resistor, and output voltage, respectively. The mathematical modeling of this converter is determined using KCL and KVL for a particular condition of the converter (Joseph and Kumar, 2012). Because it uses switches, the converter will operate in two modes: closed switch and open switch (Tan and Hoo 2015).

When the switch is closed, as shown in **Figure 3**, the inductor L will store energy via V_i. In this operation, the resistor and capacitor will not have a current flowing. During this state, the mathematical modeling of this converter can be formulated in **Eqs 1**, **2**.

$$V_i = L\frac{di_L}{dt} \tag{1}$$

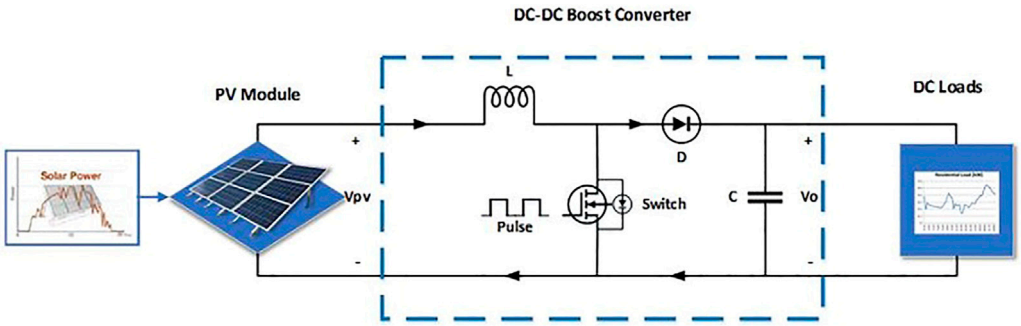

FIGURE 1 | Structure of PV energy system.

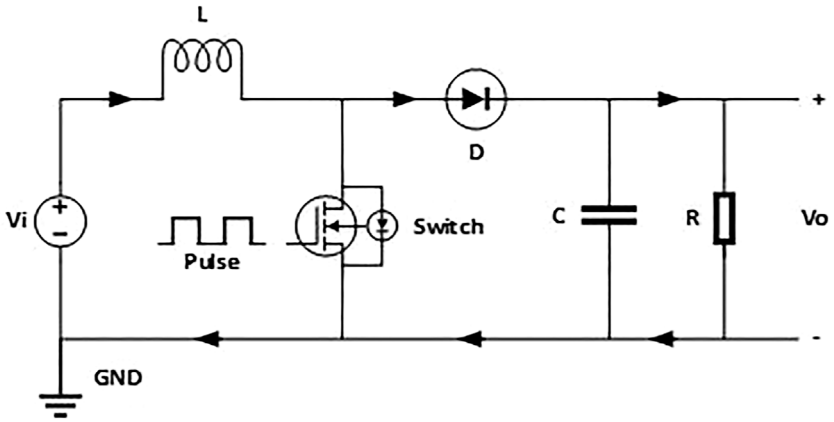

FIGURE 2 | Circuit of DC-DC boost converter.

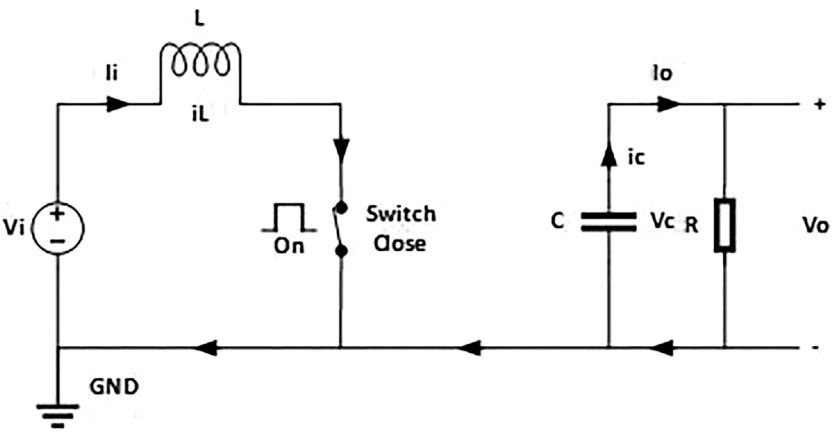

FIGURE 3 | Circuit of DC-DC in closed-switch mode.

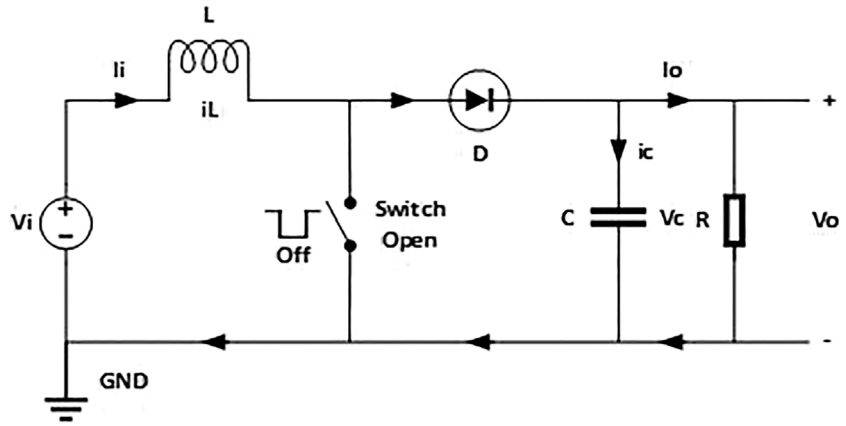

FIGURE 4 | Circuit of DC-DC in open-switch mode.

$$C\frac{dV_c}{dt} + \frac{V_c}{R} = 0 \tag{2}$$

For the open switch, as seen in **Figure 4**, the inductor L will release energy. The mathematical expression of this converter is defined in **Eqs 3**, **4**.

$$V_i = L\frac{di_L}{dt} + V_c \tag{3}$$

$$i_L - C\frac{dV_c}{dt} = \frac{V_c}{R} \tag{4}$$

By taking the state variable of the current inductor $i_L = x_1$ and voltage of the capacitor $V_c = x_2$ in **Eqs 1**–**4**, and using the average of two operation modes, the mathematical modeling of the converter can be defined in **Eq. 5**.

$$\dot{x}_1 = -\frac{(1-u)}{L}x_2 + \frac{1}{L}V_i$$
$$\dot{x}_2 = \frac{(1-u)}{C}x_1 - \frac{\varphi}{C}x_2,\ \varphi = \frac{1}{R} \tag{5}$$

OBSERVER-BASED BACKSTEPPING SLIDING MODE CONTROL

In the application, we have to note that the value of the input voltage, V_i, and load resistance, R, are unknown and varied. In the literature, input voltage V_i of the DC-DC boost converter can be a DC energy source such as in PV-based microgrids. Due to the uncertainty and variation of this input, several studies have used MPPT to overcome this problem to get maximum power of the PV system. However, using the fixed step of MPPT, the output of PV will oscillate below maximum power point. Thus, the necessity of damping is required to damp the oscillation. In this study, we assume that the input voltage of the converter has used MPPT so that the output of the PV is optimum voltage. Then, the non-linear observer controller is used to estimate V_i and R. To obtain these values, the state variables x_1 and x_2 are assumed to be accessible. In this design, $\hat{V}_i$ and $\hat{\varphi}$ are the estimated values of V_i and R, respectively. Therefore, the uncertainty of input voltage and the variation of load will be included in the formula of the proposed controller. The duty ratio u is the control input to the converter. So, the observer design can be defined as follows (Oucheriah and Guo 2013):

$$\dot{\hat{x}}_1 = -\frac{(1-u)}{L}\hat{x}_2 + \frac{\hat{V}_i}{L} + K_1(x_1 - \hat{x}_1)$$
$$\dot{\hat{x}}_2 = \frac{(1-u)}{C}\hat{x}_1 - \frac{\hat{\varphi}}{C}x_2 + K_2(x_2 - \hat{x}_2) \tag{6}$$

$K_1 > 0$ and $K_2 > 0$ represent the gain of the observer. $\hat{x}_1$ and $\hat{x}_2$ represent the estimate of x_1 and x_2, respectively. Assuming $\tilde{x}_1 = x_1 - \hat{x}_1$, $\tilde{x}_2 = x_2 - \hat{x}_2$, $\tilde{\varphi} = \varphi - \hat{\varphi}$, and $\tilde{V}_i = V_i - \hat{V}_i$, then, using **Eqs 5**, **6**, we get the following expression:

$$\dot{\tilde{x}}_1 = -\frac{(1-u)}{L}\tilde{x}_2 + \frac{\tilde{V}_i}{L} + K_1\tilde{x}_1$$
$$\dot{\tilde{x}}_2 = \frac{(1-u)}{C}\tilde{x}_1 - \frac{\tilde{\varphi}}{C}x_2 + K_2\tilde{x}_2 \tag{7}$$

To obtain the adaptation laws, the quadratic Lyapunov function is considered.

$$V = \frac{1}{2}\left(L\tilde{x}_1^2 + C\tilde{x}_2^2 + \frac{1}{\gamma_1}\tilde{\varphi}^2 + \frac{1}{\gamma_2}\tilde{V}_i^2\right) \tag{8}$$

The gains of adaptation are represented by $\gamma_1 > 0$ and $\gamma_2 > 0$. Then, its time derivative, as in **Eq. 8**, leads to the formulation as follows:

$$\dot{V} = -K_1L\tilde{x}_1^2 - K_2C\tilde{x}_2^2 - \tilde{\varphi}\left(x_2\tilde{x}_2 + \frac{1}{\gamma_1}\dot{\hat{\varphi}}\right) + \tilde{V}_i\left(\tilde{x}_1 - \frac{1}{\gamma_2}\dot{\hat{V}}_i\right) \tag{9}$$

For stabilization of the observer design, (9) should be negative definite; hence, the terms in the bracket must be cancelled to obtain the adaptation laws in **Eqs 10**, **11**.

$$\dot{\hat{\varphi}} = -\gamma_1 x_2\tilde{x}_2 \tag{10}$$

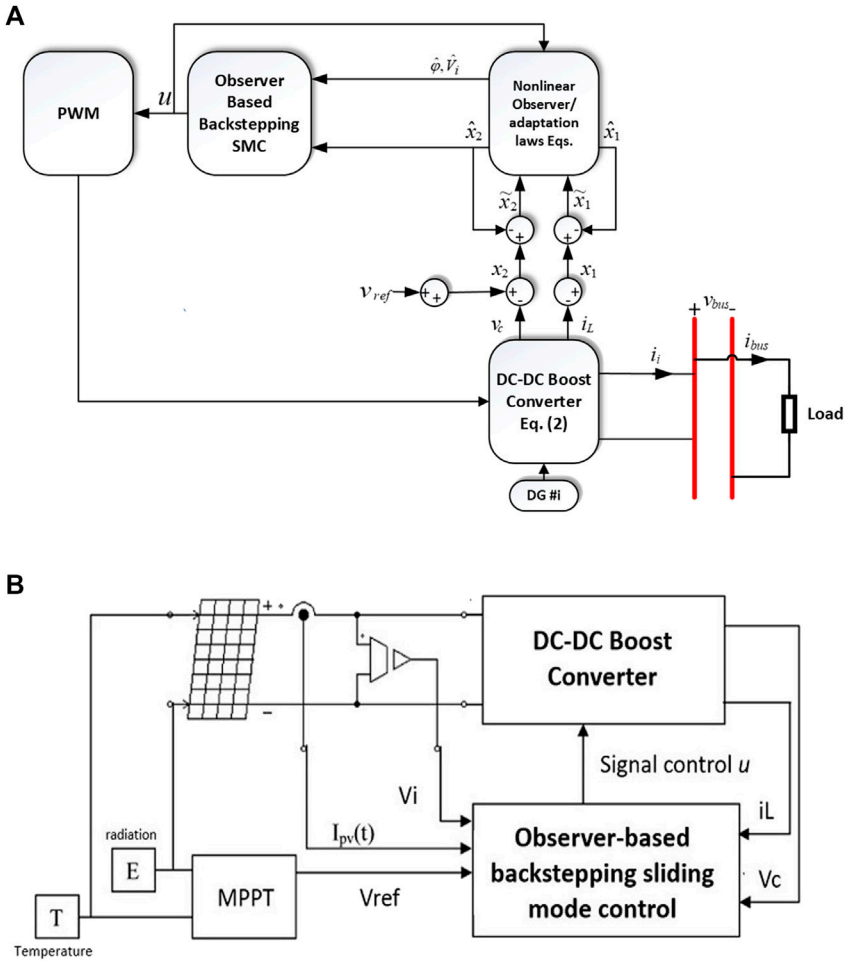

FIGURE 5 | Block diagram of the proposed system **(A)** implemented for DC microgrid; **(B)** implemented for PV system with MPPT.

$$\dot{\hat{V}}_i = \gamma_2 \tilde{x}_1 \tag{11}$$

Because the DC-DC boost converter has non-minimum phase characteristics, an indirect control method must be used. For this condition, the voltage of the system output should be regulated using its inductor current. The reference of the inductor current I_{Lref} is determined using the following equation:

$$I_{Lref} = \frac{V_{ref}^2}{\hat{V}_i}\hat{\varphi} \tag{12}$$

where V_{ref} is the reference voltage. The sliding surface for static PI is simply constructed as

$$\sigma = e + \lambda \int e\, dt \tag{13}$$

where $e = \hat{x}_1 - I_{Lref}$ and λ is the parameter of the switching surface.

To provide robustness and to ensure the stability of the system, the backstepping method is added into the observer-based SMC. The main idea of the backstepping method is that a complex non-linear system is divided into two subsystems. Consequently, the medial fictitious control and Lyapunov function are constructed, respectively, and the main system is gained through backstepping. The design procedure of the basic OBSMC can be defined as follows:

There are two steps to designing the OBSMC. The first step is to select the Lyapunov function as

$$V_1 = \frac{1}{2}e^2 \tag{14}$$

Accordingly, $\dot{V}_1 = e\dot{e}$ and using $e = \hat{x}_1 - I_{Lref}$, $\dot{V}_1 = (\hat{x}_1 - \frac{V_{ref}^2}{\hat{V}_i}\hat{\varphi})\dot{e}$. To satisfy $\dot{V}_1 \leq 0$, we suppose $\hat{x}_1 = \sigma - \lambda \int e + \frac{V_{ref}^2}{\hat{V}_i}\hat{\varphi}$. Hence,

$$\dot{V}_1 = \dot{e}\left(\sigma - \lambda \int e\right)$$
$$\dot{V}_1 = \dot{e}\sigma - \lambda \dot{e} \int e \tag{15}$$

In the second step, the Lyapunov function is selected as

$$V_2 = V_1 + \frac{1}{2}\sigma^2 \tag{16}$$

TABLE 1 | The DC-DC boost converter and switching surface parameters.

System	Parameter	Symbol	Value	Units
Boost converter	Input DC voltage	V_i	12	V
	Inductor	L	1.5	mH
	Capacitor	C	50	μF
	Resistor load	R	200	Ω
Switching surface	Adaptation gains	γ_1	1	–
		γ_2	2.10^4	–
	Observer gains	K_1	10^4	–
		K_2	10^4	–
	Controller gain	λ	1,000	–

The time derivative of **Eq. 16** will get

$$\dot{V}_2 = \dot{V}_1 + \sigma\dot{\sigma} \tag{17}$$

Substituting (13), the derivative of **Eqs 13**, **15** into **Eq. 17** gives

$$\dot{V}_2 = \dot{e}\sigma - \lambda\dot{e}\int e + \sigma(\dot{e} + \lambda e) \tag{18}$$

To meet $\dot{V}_2 \leq 0$, a controller will be designed based on the time derivative of **(9)** and substituting (2) into it.

$$u = 1 - \frac{L}{\hat{x}_2}\left(\frac{\hat{V}_i}{L} + K_1\tilde{x}_1 + \frac{\gamma_1 V_{ref}^2}{\hat{V}_i}x_2\tilde{x}_2 + \frac{\gamma_2 V_{ref}^2}{\hat{V}_i^2}\hat{\varphi}\tilde{x}_1 + \lambda e\right) - \frac{L}{\hat{x}_2}sgn(\sigma) - \frac{L}{\hat{x}_2}\dot{e} + \frac{L}{\hat{x}_2}\frac{\lambda\dot{e}\int e}{\sigma} \tag{19}$$

The block diagram of the proposed system using signal control **Eq. 19** is presented in **Figure 5A**. The proposed system does not need an inductor current sensor. To replace the sensor and to obtain the estimation value of inductor current accurately, the input and output voltage are fed to the observer gained as in **Eq. 6**. The estimated values of the inductor current and the output voltage are used to design the purposed controller. The control signal in **(19)**, which is a gating signal to drive the MOSFET, is generated by the purposed controller such that the output voltage can reach the reference voltage as close as possible although disturbance appears in the system.

SIMULATION RESULT AND DISCUSSION

To verify the performance of the proposed controller, a numerical simulation has been performed using MATLAB Simulink. The DC-DC boost converter and switching surface parameters utilized in this paper are provided in **Table 1**. For the initial system simulation, V_{ref} is selected as 24 V. To guarantee the existence of the sliding mode control, the initial conditions selected for the system are as follows: $\hat{x}_1(0) = 0.8, \hat{x}_2(0) = 6, \hat{V}_i(0) = 10\ \hat{\varphi}(0) = 0.0048$.

In this paper, the proposed controller, OBSMC, is compared with observer-based SMC (OSMC) in Pandey et al. (2018). Three types of system testing are employed in this paper. The first system testing is reference voltage changing. The simulation time is set to be 0.15 s. In addition, to evaluate the performance quality of the controller, integral absolute error (IAE) is utilized. IAE is the sum of the areas below and above the reference signal and process value. At the beginning of the simulation, reference voltage, V_{ref}, is set as 24 V. Then, at $t = 0.05$ s, V_{ref} is decreased to 20 V and at $t = 0.1$ s, V_{ref} is increased to 24 V. **Figure 6** presents the comparison of converter output voltage regarding voltage variation between OBSMC and OSMC. It can be seen that the performance of the OBSMC is better than OSMC in terms of overshoot and transient response. In the starting condition, there is no overshoot for the proposed controller

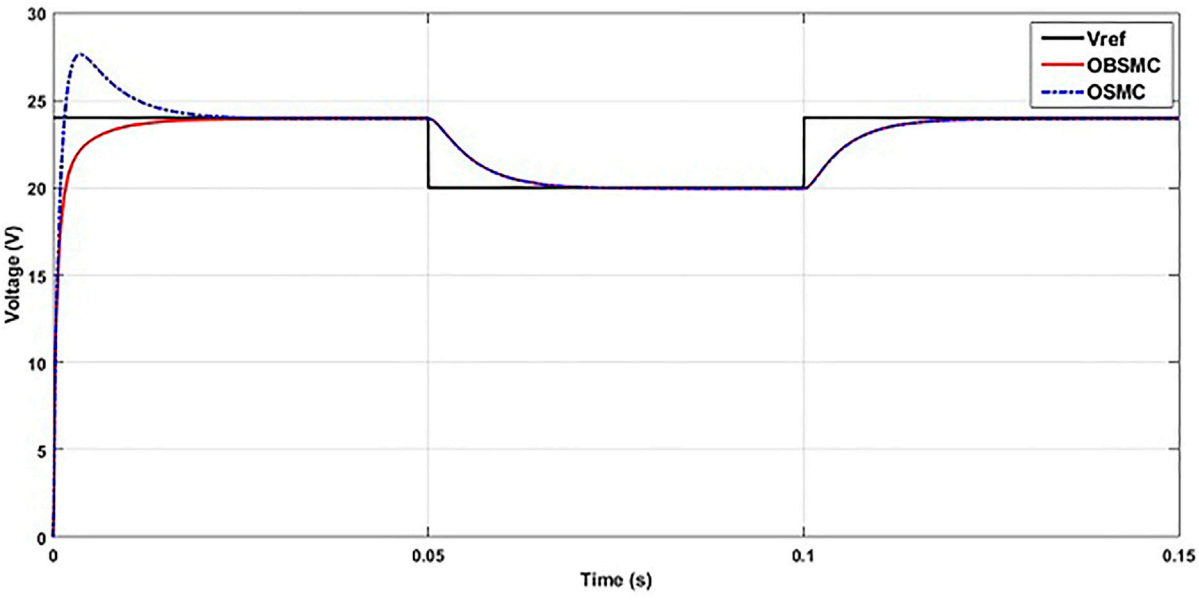

FIGURE 6 | Output voltage of the converter for reference voltage variations.

TABLE 2 | Performance specification of the converter related to reference voltage variations

Controller	Starting		Decreasing		Increasing		IAE
			V_{ref} (−4 V)		V_{ref} (+4 V)		
	ΔV (V)	t_s (ms)	ΔV (V)	t_s (ms)	ΔV (V)	t_s (ms)	
OBSMC	0	5.38	0	58.07	0	107.1	0.0826
OSMC	27.62	9.25	0	58.07	0	107.1	0.0916

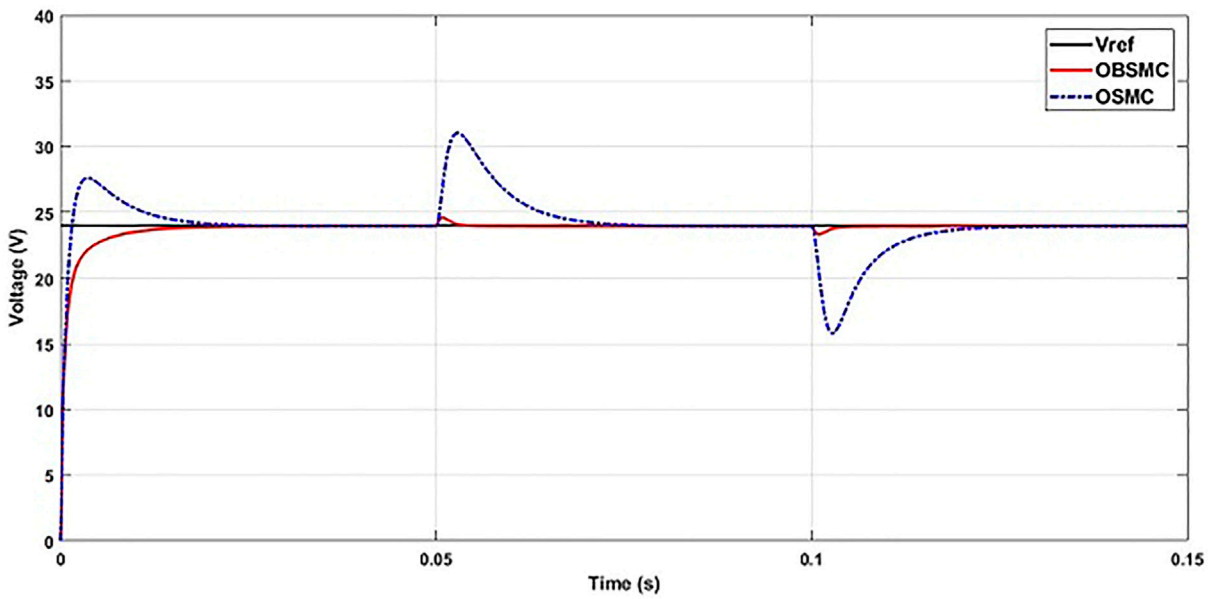

FIGURE 7 | Output voltage of the converter for input voltage variations.

TABLE 3 | Performance specification of the converter related to input voltage variations

Controller	Increasing V_i (+2 V)		Decreasing V_i (−2 V)		IAE
	ΔV (V)	t_{rec} (ms)	ΔV (V)	t_{rec} (ms)	
OBSMC	0.59	1.4	0.67	1.7	0.0396
OSMC	7.03	17.56	8.2	17	0.1558

OBSMC, but for the OSMC, the overshoot occurs around 27.62 V. Thereafter, at $t = 0.05$ s, when V_{ref} is decreased, both OBSMC and OSMC have the same performance. The same performance of both controllers occurs at $t = 0.1$ s when V_{ref} is increased to 24 V. To evaluate the performance quality, IAE is used. It can be seen that the IAE of the proposed controller OBSMC, 0.0826, is smaller than that of OSMC, 0.0916. Therefore, through system testing, the results show that the proposed controller OBSMC provides less steady-state error, small overshoot, and fast transient response. The detailed information regarding the performance specification of the response is provided in **Table 2**.

The next system testing is the input voltage variation V_i. The simulation time is set to be 0.15 s. The input voltage, V_i, is set as 12 V at the beginning of the simulation. Then, at $t = 0.05$ s, V_i is reduced to 8 V and $t = 0.1$ s; V_i is then raised and reduced back to 12 V. The comparison of the converter output voltage with the input voltage variation V_i between OBSMC and OSMC is shown in **Figure 7**. It can be seen clearly that the performance of the OBSMC is better than OSMC in terms of robustness and fast recovery time. At $t = 0.05$ s, when the input voltage variation V_i is raised, the voltage deviation of OBSMC is smaller at 0.59 V than OSMC at 7.03 V. Moreover, the recovery time of OBSMC is smaller at 1.4 ms than OSMC at 17.56 ms. Then, V_i is reduced at $t = 0.1$ s. In this condition, the voltage deviation of OBSMC is smaller at 0.67 V than OSMC at 8.2 V. The recovery time of OBSMC is ten times smaller at 1.7 ms than OSMC at 17 ms. IAE is also used to evaluate the performance quality of the proposed controller. The IAE of the proposed controller OBSMC, at 0.0396, is smaller than OSMC, at 0.1558. Thus, using this system testing shows that the proposed controller OBSMC provides a more robust and faster recovery time. The detailed information regarding the performance specification of the response is provided in **Table 3**. Another input voltage, V_i, testing for greatly varied values is applied to the system. The variation of V_i is appropriate to the real system. **Figure 8** depicts the output voltage of the converter with a greatly varied value of V_i. The

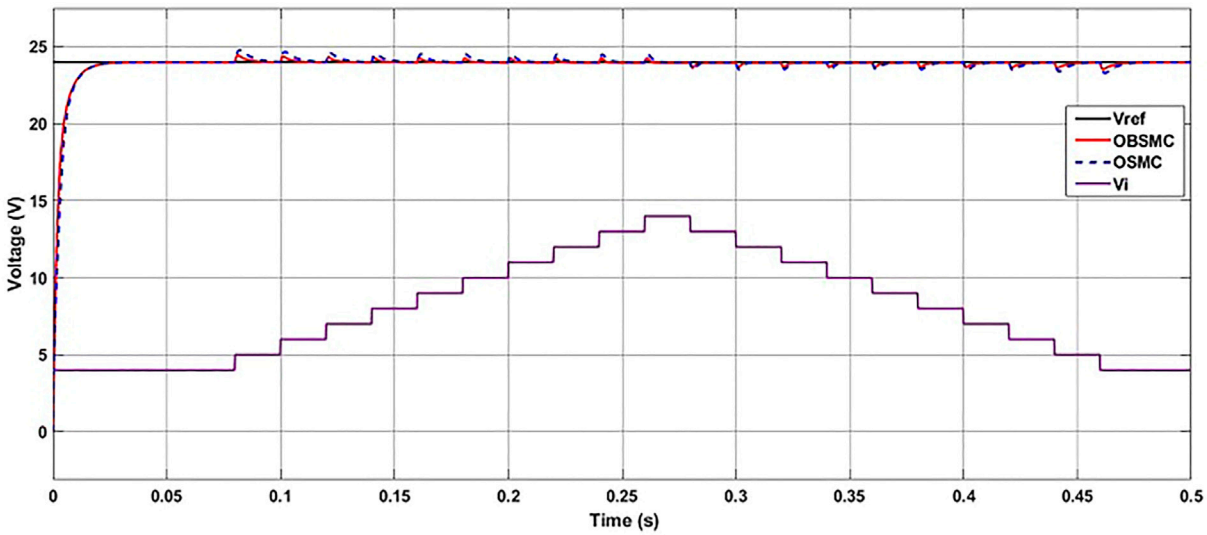

FIGURE 8 | The output voltage of the converter with the greatly varied value of input voltage V_i

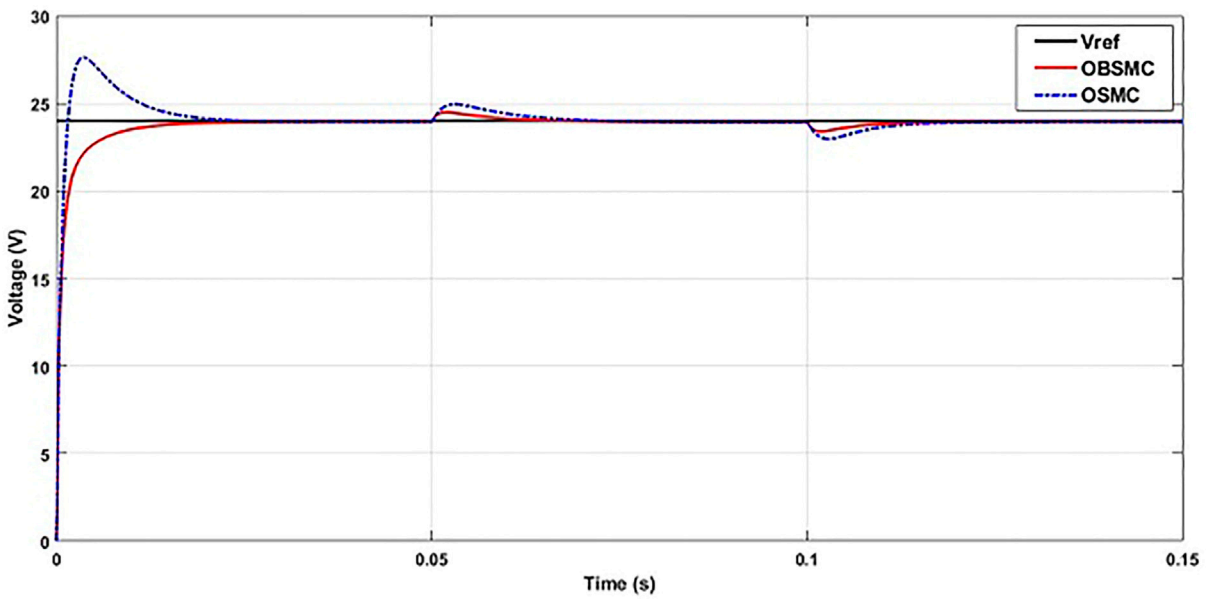

FIGURE 9 | Output voltage of the converter for load resistance variations.

characteristic of the PV output real data is obtained from Kaddoura et al. (2016) with the change in range of the time. Using IAE, the proposed controller OBSMC has less IAE, 0.1023, than the OSMC, 0.1345.

The last system testing is the load resistance variation. The simulation time is set to be 0.15 s. Initially, R is set to be 200 Ω. Afterwards, at $t = 0.05$ s, R is increased +50%, and at $t = 0.1$ s, R is decreased by 50%. The comparison of the converter output voltage with load resistance variation between OBSMC and OSMC is shown

TABLE 4 | Performance specification of the converter related to load resistance variations

Controller	Increasing R (+50%)		Decreasing R (−50%)		IAE
	ΔV (V)	t_{rec} (ms)	ΔV (V)	t_{rec} (ms)	
OBSMC	0.5	2.2	0.6	3.8	0.0438
OSMC	0.96	9.03	1.03	8.3	0.0618

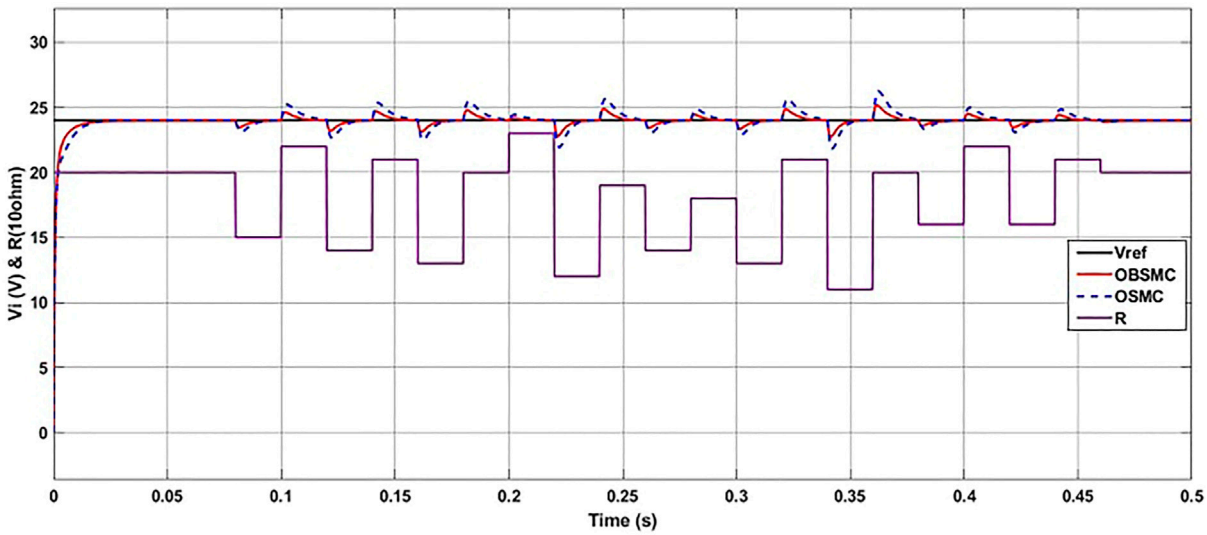

FIGURE 10 | Output voltage of the converter for load resistance variation*R*.

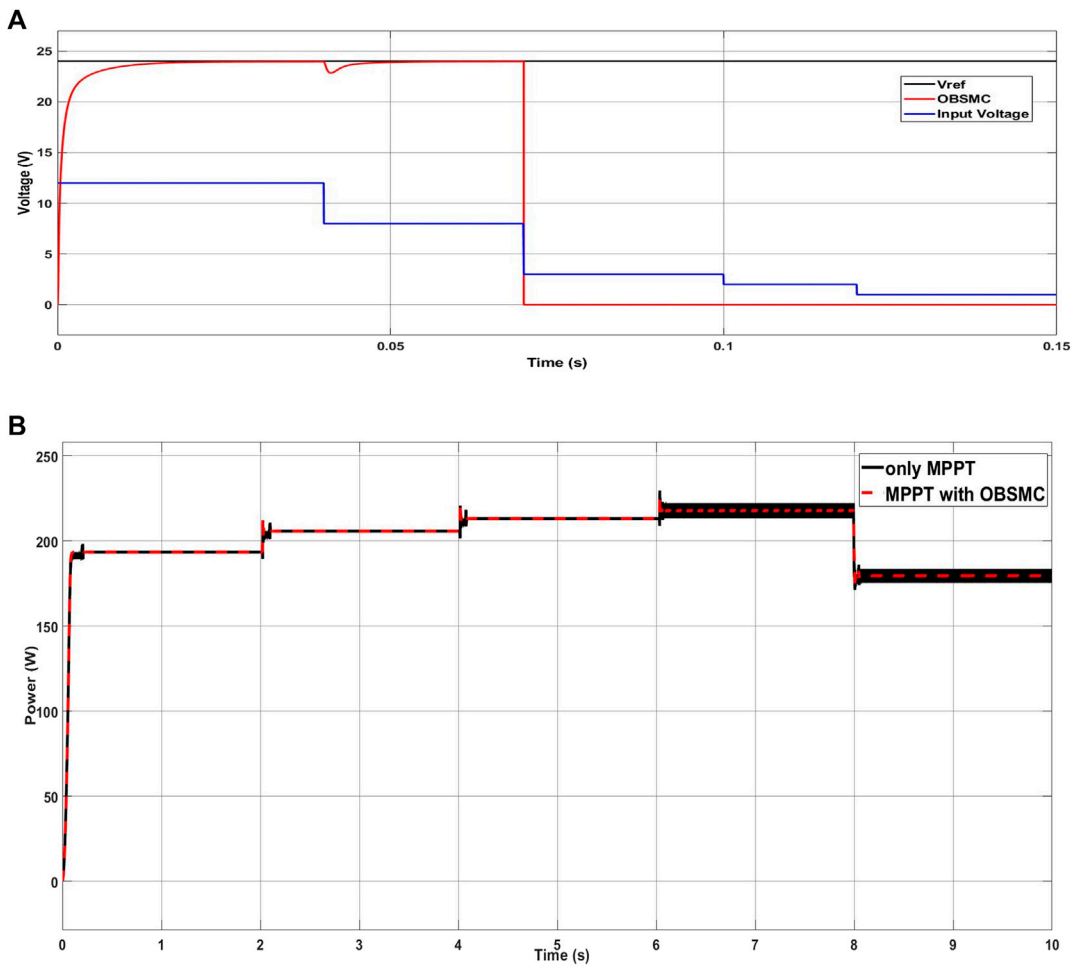

FIGURE 11 | Output of the converter for **(A)** efficient operation and **(B)** for MPPT implementation.

in **Figure 9**. The performance of the OBSMC is better than OSMC in terms of robustness and fast recovery time. At $t = 0.05$ s, when the load resistance variation R is raised, the voltage deviation of OBSMC is smaller (0.59 V) than OSMC (0.95 V). In addition, the recovery time of OBSMC is less (2.2 ms) than that of OSMC (9.03 ms). Next, load resistance variation R is reduced at $t = 0.1$ s. In this condition, the voltage deviation of OBSMC is smaller, 0.6 V, than OSMC, 1.03 V. Furthermore, the recovery time of OBSMC is ten times smaller, 3.8 ms, than OSMC, 8.3 ms. IAE is also used to evaluate the performance quality of the purposed controller. It can be seen that the IAE of the proposed controller OBSMC, 0.0438, is smaller than that of OSMC, 0.0618. Thus, using this system testing shows that the proposed controller OBSMC provides a more robust and faster recovery time. **Table 4** presents detailed information regarding the performance specification of the response. Another load resistance variation R testing for greatly varied values is applied to the system; R is proper with the real system. **Figure 10** shows the output voltage of the converter with the greatly varied value of load resistance variation, R. It can be seen that the performance of the proposed controller OBSMC is better than OSMC. Moreover, by using IAE, the proposed controller OBSMC has less IAE, 0.1162, than the OSMC, 0.2097.

To avoid low efficient operations, the proposed controller has been evaluated with minimum input voltage of the DC-DC boost converter. We assume that if PV is considered as DC source of the system, the minimum solar irradiation will produce minimum output voltage of PV, which is 3 V. Therefore, if the input of the converter $V_i \leq 3$, the proposed controller will be off so that there is no signal control to the converter and the output of the converter will be 0 V. The output of the converter for efficient operation is shown in **Figure 11A**. At the beginning of the simulation, the simulation time is set to be 0.15 s. Initially, the input voltage V_i is set as 12 V. Then, at $t = 0.04$ s, V_i is reduced to 8 V. The system is still on so that the controller can make the output voltage return to its reference value. Then at $t = 0.7$, $t = 0.1$, and $t = 0.12$, V_i is reduced to 3 V, 2 V, and 1 V, respectively. In these conditions, the output of the converter is 0 V since the input of the converter $V_i \leq 3$ and the system is off. As a result, the proposed controller can turn off when the solar irradiation is too low to avoid low efficient operations.

Another implementation of the proposed controller is to control the optimal output of the PV system. Due to variation of solar irradiation and temperature, a MPPT is required to run the PV system at maximum power point (MPP) (Nguyen et al., 2020). The MPPT algorithm employed in this study is based on perturb and observe (P&O) method. As proposed by Dahech et al. (2017), in this study, the output of the MPPT system is used as a voltage reference to the proposed controller, that is, OBSMC. The signal control of OBSMC is then utilized to regulate the switching device. **Figure 5B** shows the structure of the MPPT system and the proposed controller applied in the PV system. The output power of DC-DC boost converter with MPPT and the proposed controller is presented in **Figure 11B**. In this implementation, the performance of the MPPT system with OBSMC and without OBSMC is compared. In the beginning, solar irradiation is 200 W/m^2 and the temperature value is 25°C. At $t = 2$ s, 4 s, and 6 s, the solar irradiation is increased to 400 W/m^2, 600 W/m^2, and 800 W/m^2, respectively. Then, at $t = 8$ s, the temperature value is changed to 50°C. As can be seen in **Figure 11B**, at $t = 2$ s, 4 s, 6 s, and 8 s, the output power of the converter is 193.45, 205.74, 213.11, and 179.66 W, respectively, for only MPPT and MPPT with OBSMC. There is a short oscillation for systems that use only MPPT at $t = 2$ and 4 s and a long oscillation at $t = 6$ s and 8 s whereas there is no oscillation for system using MPPT with OBSMC at all t.

CONCLUSION

This paper presents observer-based backstepping SMC considering load variation and input voltage uncertainty to regulate a DC-DC boost converter. The backstepping technique has been combined with the SMC to make the controller more robust and have a less steady-state error, small overshoot, a fast recovery time, and fast transient response time. Moreover, the Lyapunov direct method was employed to ensure the stability of the proposed method. To verify the performance of the proposed controller, the numerical simulation is performed using MATLAB Simulink. There were three types of system testing employed in this paper, namely, the reference voltage V_{ref} changing, the input voltage variation, V_i, and the load resistance variation, R. The simulation results show that the proposed controller OBSMC provides less steady-state error, smaller overshoot, and a faster transient response time than OSMC when the system is tested by the reference voltage, V_{ref}, changing. Using the input voltage variation, V_i, and the load resistance variation, R, the recovery time of OBSMC was faster than OSMC and the voltage deviation was smaller. In addition, the proposed method consistently produced the least value of IAE in all system testing. In the last part of this paper, an analysis of the proposed controller equipped with an MPPT controller was conducted. It is concluded that there is no power oscillation for the system using MPPT with OBSMC at all t.

DATA AVAILABILITY STATEMENT

The original contributions presented in the study are included in the article/Supplementary Material, further inquiries can be directed to the corresponding author.

AUTHOR CONTRIBUTIONS

The main idea, simulation, analysis, and writing of this work was provided by RM. MS and FB carried out a literature review, overall layout formatting, and proof-reading while MAR and HB provided substantial and intellectual contribution. Revision of the article was carried out by RM, AM, and MR. All authors listed have approved the submitted version of the article.

FUNDING

The authors extend their appreciation to the Deputyship for Research and Innovation, Ministry of Education in Saudi Arabia for funding this research work through the project number IFPRC-190-135-2020 and King Abdulaziz University, DSR, Jeddah, Saudi Arabia.

REFERENCES

Abdelmalek, S., Dali, A., Bakdi, A., and Bettayeb, M. (2020). Design and Experimental Implementation of a New Robust Observer-Based Nonlinear Controller for DC-DC Buck Converters. *Energy* 213, 118816. doi:10.1016/j.energy.2020.118816

Abhinav, S., Modares, H., Lewis, F. L., and Davoudi, A. (2019). Resilient Cooperative Control of DC Microgrids. *IEEE Trans. Smart Grid* 10 (1), 1083–1085. doi:10.1109/tsg.2018.2872252

Alawieh, A., Ortega, R., Pillai, H., Astolfi, A., and Berthelot, E. (2011). "Adaptive Control of the Boost Converter in Discontinuous Conduction Mode," in IFAC Proceedings Volumes (IFAC-PapersOnline), Milano, Italy, January 2011. doi:10.3182/20110828-6-it-1002.03558

Alsolami, M. (2021). A Multi-Input, Multi-Stage Step-Up DC-DC Converter for PV Applications. *Alexandria Eng. J.* 60 (2), 2315–2324. doi:10.1016/j.aej.2020.12.030

Amirabadi, M. (2016). "Ćuk-Based Universal Converters in Discontinuous Conduction Mode of Operation," in ECCE 2016 - IEEE Energy Conversion Congress and Exposition, Milwaukee, WI, USA, 18-22 Sept. 2016. doi:10.1109/ecce.2016.7854978

Arun, S., and Manigandan, T. (2021). Design of ACO Based PID Controller for Zeta Converter Using Reduced Order Methodology. *Microprocessors and Microsystems* 81, 103629. doi:10.1016/j.micpro.2020.103629

Balog, R. S., Weaver, W. W., and Krein, P. T. (2012). The Load as an Energy Asset in a Distributed DC Smartgrid Architecture. *IEEE Trans. Smart Grid* 3 (1), 253–260. doi:10.1109/tsg.2011.2167722

Basharat, S., Awan, S. E., Akhtar, R., Hussain, A., Iqbal, S., Shah, S. A., et al. (2021). A Duty Cycle Controlled ZVS Buck Converter with Voltage Doubler Type Auxiliary Circuit. *Front. Energ. Res.* 9. doi:10.3389/fenrg.2021.550115

Bjaoui, M., Khiari, B., Benadli, R., Memni, M., and Sellami, A. (2019). Practical Implementation of the Backstepping Sliding Mode Controller MPPT for a PV-Storage Application. *Energies* 12 (18), 3539. doi:10.3390/en12183539

Bouchekara, H. R. E-H., Javaid, M. S., Shaaban, Y. A., Shahriar, M. S., Ramli, M. A. M., and Latreche, Y. (2021). Decomposition Based Multiobjective Evolutionary Algorithm for PV/Wind/Diesel Hybrid Microgrid System Design Considering Load Uncertainty. *Energ. Rep.* 7, 52–69. doi:10.1016/j.egyr.2020.11.102

Cajamarca, B., Quintero, Ó. C., Chávez, D., Leica, P., and Pozo, M. (2019). Sliding Mode Control Based on Internal Model for a Non-minimum Phase Buck and Boost Converter. *Enfoque UTE* 10 (1), 41–53. doi:10.29019/enfoqueute.v10n1.442

Chen, D., Lin, Y., and Xiao, L. (2020). An EMI Filter Design Method Based on Improved Foster Network Model for Boost PFC Converter. *Energ. Rep.* 6, 1268–1275. doi:10.1016/j.egyr.2020.11.044

Cisneros, R., Pirro, M., Bergna, G., Ortega, R., Ippoliti, G., and Molinas, M. (2015). Global Tracking Passivity-Based PI Control of Bilinear Systems: Application to the Interleaved Boost and Modular Multilevel Converters. *Control. Eng. Pract.* 43, 109–119. doi:10.1016/j.conengprac.2015.07.002

Cucuzzella, M., Lazzari, R., Trip, S., Rosti, S., Sandroni, C., and Ferrara, A. (2018). Sliding Mode Voltage Control of Boost Converters in DC Microgrids. *Control. Eng. Pract.* 73, 161–170. doi:10.1016/j.conengprac.2018.01.009

Dahech, K., Allouche, M., Damak, T., and Tadeo, F. (2017). Backstepping Sliding Mode Control for Maximum Power Point Tracking of a Photovoltaic System. *Electric Power Syst. Res.* 143, 182. doi:10.1016/j.epsr.2016.10.043

Eguchi, K., Shibata, A., and Harada, Y. (2020). A Direct High Step-Down DC/DC Converter Using Cascade Ring-type Converters. *Energ. Rep.* 6, 119–124. doi:10.1016/j.egyr.2019.11.051

Farsizadeh, H., Gheisarnejad, M., Mosayebi, M., Rafiei, M., and Khooban, M. H. (2020). An Intelligent and Fast Controller for DC/DC Converter Feeding CPL in a DC Microgrid. *IEEE Trans. Circuits Syst. Express Briefs* 67 (6), 1104–1108. doi:10.1109/tcsii.2019.2928814

Guo, L., and Abdul, N. M. M. (2021). Design and Evaluation of Fuzzy Adaptive Particle Swarm Optimization Based Maximum Power Point Tracking on Photovoltaic System under Partial Shading Conditions. *Front. Energ. Res.* 9. doi:10.3389/fenrg.2021.712175

Guo, L., Hung, J. Y., and Nelms, R. M. (2011). Comparative Evaluation of Sliding Mode Fuzzy Controller and PID Controller for a Boost Converter. *Electric Power Syst. Res.* 81 (1), 99–106. doi:10.1016/j.epsr.2010.07.018

Johnson, R. S., Altin, B., and Sanfelice, R. G. (2021). Hybrid Adaptive Control for the DC-DC Boost Converter. *IFAC-PapersOnLine* 54 (5), 73–78. doi:10.1016/j.ifacol.2021.08.477

Joseph, X. F., and Kumar, S. P. (2012). Design and Simulation of a Soft Switched Dc Boost Converter for Switched Reluctance Motor. *Am. J. Appl. Sci.* 9 (3), 440–445.

Kaddoura, T. O., Ramli, M. A. M., and Al-Turki, Y. A. (2016). On the Estimation of the Optimum Tilt Angle of PV Panel in Saudi Arabia. *Renew. Sust. Energ. Rev.* 65, 626–634. doi:10.1016/j.rser.2016.07.032

Kobaku, T., Jeyasenthil, R., Sahoo, S., and Dragicevic, T. (2021a). Experimental Verification of Robust PID Controller under Feedforward Framework for a Nonminimum Phase DC-DC Boost Converter. *IEEE J. Emerging Selected Top. Power Elect.* 9 (3), 3373–3383. doi:10.1109/jestpe.2020.2999649

Kobaku, T., Jeyasenthil, R., Sahoo, S., Ramchand, R., and Dragicevic, T. (2021b). Quantitative Feedback Design-Based Robust PID Control of Voltage Mode Controlled DC-DC Boost Converter. *IEEE Trans. Circuits Syst. Express Briefs* 68 (1), 286–290. doi:10.1109/tcsii.2020.2988319

Li, G., Huang, H., Song, S., and Liu, B. (2021). A Nonlinear Control Scheme Based on Input–Output Linearized Method Achieving PFC and Robust Constant Voltage Output for Boost Converters. *Energ. Rep.* 7, 5386–5393. doi:10.1016/j.egyr.2021.08.169

Liu, L., Zhao, Y., Chang, D., Xie, J., Ma, Z., Sun, Q., et al. (2018). Prediction of Short-Term PV Power Output and Uncertainty Analysis. *Appl. Energ.* 228, 700–711. doi:10.1016/j.apenergy.2018.06.112

Mahajan, T., and Potdar, M. S. (2020). "An Improved Strategy for Distributed Generation Control and Power Sharing in Islanded Microgrid," in 2nd International Conference on Innovative Mechanisms for Industry Applications, ICIMIA 2020, Bangalore, India, 5-7 March 2020, 133–136.

Martínez-Treviño, B. A., Jammes, R., El Aroudi, A., and Martínez-Salamero, L. (2017). Sliding-Mode Control of a Boost Converter Supplying a Constant Power Load. *IFAC-PapersOnLine* 50 (1), 7807–7812. doi:10.1016/j.ifacol.2017.08.1055

Mehdi, M., Kim, C.-H., and Saad, M. (2020). Robust Centralized Control for DC Islanded Microgrid Considering Communication Network Delay. *IEEE Access* 8, 77765–77778. doi:10.1109/access.2020.2989777

Mehreganfar, M., Saeedinia, M. H., Davari, S. A., Garcia, C., and Rodriguez, J. (2019). Sensorless Predictive Control of Afe Rectifier with Robust Adaptive Inductance Estimation. *IEEE Trans. Ind. Inf.* 15 (6), 3420–3431. doi:10.1109/tii.2018.2879060

Mobayen, S., and Tchier, F. (2018). Robust Global Second-Order Sliding Mode Control with Adaptive Parameter-Tuning Law for Perturbed Dynamical Systems. *Trans. Inst. Meas. Control.* 40 (9), 2855–2867. doi:10.1177/0142331217708832

Mohamed, A. T., Mahmoud, M. F., Swief, R. A., Said, L. A., and Radwan, A. G. (2021). Optimal Fractional-Order PI with DC-DC Converter and PV System. *Ain Shams Eng. J.* 12 (2), 1895. doi:10.1016/j.asej.2021.01.005

Mushi, A., Nagai, S., Obara, H., and Kawamura, A. (2017). Fast and Robust Nonlinear Deadbeat Current Control for Boost Converter. *IEEJ J. Industry Appl.* 6 (5), 311–319. doi:10.1541/ieejjia.6.311

Nguyen, B. N., Nguyen, V. T., Duong, M. Q., Le, K. H., Nguyen, H. H., and Doan, A. T. (2020). Propose a MPPT Algorithm Based on Thevenin Equivalent Circuit for Improving Photovoltaic System Operation. *Front. Energ. Res.* 8. doi:10.3389/fenrg.2020.00014

Nizami, T. K., and Chakravarty, A. (2020). Neural Network Integrated Adaptive Backstepping Control of DC-DC Boost Converter. *IFAC-PapersOnLine* 53 (1), 549–554. doi:10.1016/j.ifacol.2020.06.092

Oucheriah, S., and Guo, L. (2013). PWM-based Adaptive Sliding-Mode Control for Boost DC-DC Converters. *IEEE Trans. Ind. Elect.* 60 (8), 3291–3294. doi:10.1109/tie.2012.2203769

Pandey, S. K., Patil, S. L., and Phadke, S. B. (2018). Comment on PWM-Based Adaptive Sliding-Mode Control for Boost DC-DC Converters. *IEEE Trans. Ind. Elect.* 65 (6), 5078–5080. doi:10.1109/tie.2017.2764872

Pandey, S. K., Veeranna, K., Patil, S. L., and Phadke, S. B. (2020). Uncertainty Estimator Based Sliding Mode Control Schemes for Multimode Noninverting Buck-Boost DC-DC Converter. *IFAC-PapersOnLine* 53 (1), 555–560. doi:10.1016/j.ifacol.2020.06.093

Premkumar, M., Kumar, C., and Sowmya, R. (2019). Analysis and Implementation of High-Performance DC-DC Step-Up Converter for Multilevel Boost Structure. *Front. Energ. Res.* 7. doi:10.3389/fenrg.2019.00149

Ramos-Paja, C. A., Montoya, D. G., and Bastidas-Rodríguez, J. D. (2020). Sliding-Mode Control of a CuK Converter for Voltage Regulation of a Dc-Bus. *Sustainable Energ. Tech. Assessments* 42, 100807. doi:10.1016/j.seta.2020.100807

Saveen, G., Raju, P. P., Manikanta, D. V., and Praveen, M. S. (20182018). Design and Implementation of Energy Management System with Fuzzy Control for Multiple Microgrid. *Proc. 2nd Int. Conf. Inventive Syst. Control ICISC* 28 (4), 1239–1244. doi:10.1109/icisc.2018.8399003

Shen, H., Tao, P., Lyu, R., Ren, P., Ge, X., and Wang, F. (2021). Risk-Constrained Optimal Bidding and Scheduling for Load Aggregators Jointly Considering Customer Responsiveness and PV Output Uncertainty. *Energ. Rep.* 7, 4722–4732. doi:10.1016/j.egyr.2021.07.021

Tahri, A., El Fadil, H., Rachid, A., Eric, M., and Giri, F. (2019). A Nonlinear Controller Based on a High Gain Observer for a Cascade Boost Converter in a Fuel Cell Distributed Power Supply System. *IFAC-PapersOnLine* 52 (29), 91–96. doi:10.1016/j.ifacol.2019.12.627

Tan, R. H. G., and Hoo, L. Y. H. (2015). "DC-DC Converter Modeling and Simulation Using State Space Approach," in 2015 IEEE Conference on Energy Conversion, CENCON, Johor Bahru, Malaysia, 19-20 Oct. 2015.

Toumi, D., Benattous, D., Ibrahim, A., Abdul-Ghaffar, H. I., Obukhov, S., Aboelsaud, R., et al. (2021). Optimal Design and Analysis of DC–DC Converter with Maximum Power Controller for Stand-Alone PV System. *Energ. Rep.* 7, 4951–4960. doi:10.1016/j.egyr.2021.07.040

Van, T. H., et al. (2021). Improving the Output of DC-DC Converter by Phase Shift Full Bridge Applied to Renewable Energy. *Rev. Roum. Si. Techn.-Electrotechn. Energ* 66 (3).

Vazquez, S., Rodriguez, J., Rivera, M., Franquelo, L. G., and Norambuena, M. (2017). Model Predictive Control for Power Converters and Drives: Advances and Trends. *IEEE Trans. Ind. Elect.* 64 (2), 935–947. doi:10.1109/tie.2016.2625238

Villegas-Ruvalcaba, M., Gurubel-Tun, K. J., and Coronado-Mendoza, A. (2021). Robust Inverse Optimal Control for a Boost Converter. *Energies* 14 (9), 2507. doi:10.3390/en14092507

Wei, M., Lin, S., Zhao, Y., Wang, H., and Liu, Q. (2021). An Adaptive Sliding Mode Control Based on Disturbance Observer for LFC. *Front. Energ. Res.* 9. doi:10.3389/fenrg.2021.733910

Wu, J., and Lu, Y. (2019). Adaptive Backstepping Sliding Mode Control for Boost Converter with Constant Power Load. *IEEE Access* 7, 50797–50807. doi:10.1109/access.2019.2910936

Xu, D., Wang, G., Yan, W., and Yan, X. (2019). A Novel Adaptive Command-Filtered Backstepping Sliding Mode Control for PV Grid-Connected System with Energy Storage. *Solar Energy* 178, 222–230. doi:10.1016/j.solener.2018.12.033

Yang, M., Wang, J., and An, J. (2020). Day-Ahead Optimization Scheduling for Islanded Microgrid Considering Units Frequency Regulation Characteristics and Demand Response. *IEEE Access* 8, 7093–7102. doi:10.1109/access.2019.2963335

Yu, D., Iu, H. H. C., Chen, H., Rodriguez, E., Alarcón, E., and El Aroudi, A. (2012). Instabilities in Digitally Controlled Voltage-Mode Synchronous Buck Converter. *Int. J. Bifurcation Chaos* 22 (1), 1250012. doi:10.1142/s0218127412500125

Yuan, X., Cheng, L., and Wei, X. (2015). Control Strategy for Boost Converter Based on Passive Sliding Control Mode. *IFAC-PapersOnLine* 48 (28), 134–137. doi:10.1016/j.ifacol.2015.12.113

Zhang, M., Li, X., Liu, J., and Su, H. (2017). Dual-Mode LQR-Feedforward Optimal Control for Non-minimum Phase Boost Converter. *IET Power Elect.* 10 (1), 92–102. doi:10.1049/iet-pel.2016.0234

Conflict of Interest: The authors declare that the research was conducted in the absence of any commercial or financial relationships that could be construed as a potential conflict of interest.

Publisher's Note: All claims expressed in this article are solely those of the authors and do not necessarily represent those of their affiliated organizations, or those of the publisher, the editors, and the reviewers. Any product that may be evaluated in this article, or claim that may be made by its manufacturer, is not guaranteed or endorsed by the publisher.